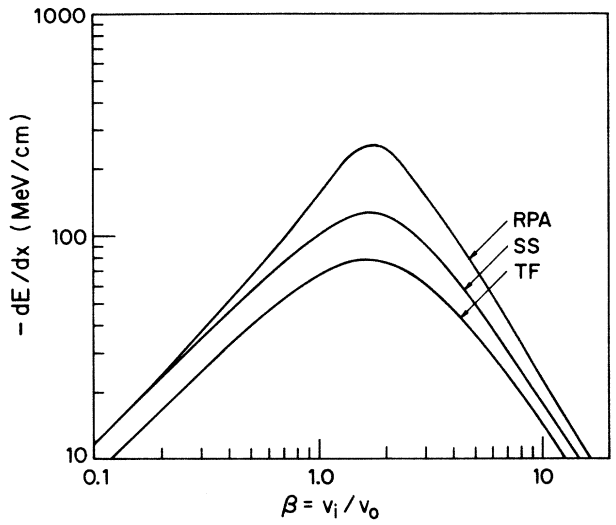

FIG. 2. Proton energy loss for $n_e = 10^{23}$ cm^{-3} as a function of velocity ratio β for three methods of calculation: dynamical screening (RPA), static self-consistent screening (SS), and Thomas-Fermi static screening (TF).

barns, it is clear that electrons dominate the slowing-down process for densities much below 10^{27} cm^{-3}, but become negligible for densities much above 10^{28} cm^{-3}. Somewhere between these two values lies the critical density for a fusion chain reaction. Detailed numerical calculations indeed confirm this estimate (the exact value depends on the fraction of the neutron energy deposited in the DT pellet, i.e., on the volume of the latter). The density required then is about 1 order of magnitude higher than densities hitherto contemplated in laser fusion. On the other hand, a high temperature is not required. Further calculations and experiments are clearly needed to decide which approach (high temperatures or high densities) is more promising.[10]

[1]E. Fermi and E. Teller, Phys. Rev. 72, 399 (1947).
[2]M. Gryziński, Phys. Rev. 111, 900 (1958).
[3]W. B. Day, J. L. Hilton, and J. L. Wyatt, Bull. Amer. Phys. Soc. 12, 760 (1967), and 13, 305 (1968).
[4]K. A. Brueckner and H. Brysk, J. Plasma Phys. 10, 141 (1973).
[5]A. A. Husseiny, Bull. Amer. Phys. Soc. 18, 1305 (1973).
[6]J. Nuckolls, L. Wood, A. Thiessen, and G. Zimmerman, Nature (London) 239, 139 (1972).
[7]J. S. Clarke, H. N. Fisher, and R. J. Mason, Phys. Rev. Lett. 30, 89 (1973).
[8]A. L. Fetter and J. D. Walecka, *Quantum Theory of Many-Particle Systems* (McGraw-Hill, New York, 1971).
[9]R. H. Ritchie, Phys. Rev. 114, 644 (1959).
[10]It is in fact quite possible that the best solution will involve some combination of both effects, because high temperatures too make an electron plasma more transparent: For slow ions, the energy loss in a nondegenerate plasma was given by S. Gasiorowicz, M. Neumann, and R. J. Riddell, Jr. [Phys. Rev. 101, (1956)] as

$$\frac{dE}{dx} = -\frac{4}{3}\left(\frac{2\pi m}{(kT)^3}\right)^{1/2} Z^2 e^4 n_e v_i \ln\left(\frac{3(kT)^{3/2}}{2Z^2 e^3 (4\pi n_e)^{1/2}}\right).$$

It appears that a fusion chain reaction may proceed in a nondegenerate DT plasma at temperatures of a few keV, at densities like those currently contemplated in laser fusion. However, larger DT pellets would be necessary to have an appreciable fraction of the 14.1-MeV neutron energy deposited in the plasma.

Infrared Conductivity of Tetrathiofulvalene Tetracyanoquinodimethane (TTF - TCNQ) Films*

D. B. Tanner, C. S. Jacobsen,† A. F. Garito, and A. J. Heeger
Department of Physics and Laboratory for Research on the Structure of Matter, University of Pennsylvania, Philadelphia, Pennsylvania 19174
(Received 4 March 1974)

Infrared studies of thin films of TTF-TCNQ are analyzed to obtain the frequency-dependent conductivity. In the metallic state the results indicate an energy gap (0.14 eV) with a collective mode at zero frequency. Below 58 K the conductivity peak moves away from zero frequency into the far infrared.

In earlier studies, it was proposed that above 58 K TTF-TCNQ is a one-dimensional (1D) metal exhibiting strong electron correlations such that the conductivity greatly exceeds the limitations of single-particle scattering.[1-4] This Letter describes infrared measurements on thin films of TTF-TCNQ which span the frequency range between the previous experiments.

We discuss the results above 58 K in terms of Fröhlich giant density fluctuations[5,6] causing the energy gap, $\hbar\omega_g = 0.14$ eV (1050 ± 100 cm^{-1}) observed in the infrared (IR). This corresponds to a mean-field Peierls temperature T_p of 400–500 K. Near 58 K, there is a metal-insulator transition to a 3D ordered state which pins[7] the conductivity and shifts it from zero frequency into the far IR.

Thin films were prepared by vacuum sublimation at 100°C of high-purity TTF-TCNQ using substrates held at 10°C by water cooling. All the starting material sublimed, leaving no residue. Film thicknesses were obtained to $\pm 25\%$ from the source-substrate configuration in the vacuum sublimator using the weight of sublimed material. Thinner films exhibited on transmission the yellow-brown color of pure TTF-TCNQ and a matte finish; thicker films were flat black. Scanning electron micrographs showed small crystals (typically, $3 \times 0.5 \times 0.1$ μm^3) growing on the substrate with random orientation. X-ray patterns showed the films had crystallized in the bulk structure; chemical analysis confirmed the 1:1 TTF-TCNQ salt.

Measurements in the range 20 to 350 cm^{-1} on films grown on sapphire or Mylar used a Grubb-Parsons Michelson interferometer. From 300 to 4000 cm^{-1}, a Perkin-Elmer 225 spectrometer was used with films grown on KBr. Film thicknesses were chosen such that transmission was always greater than 20%, i.e., 2000 Å in the near IR and 1 μm in the far IR.

The reflection and transmission coefficients of a film having conductivity $\sigma = \sigma_i - i(\omega/4\pi)(\epsilon_1 - 1)$, where σ_1 (ϵ_1) is the real part of the conductivity (dielectric function), are calculated from the boundary conditions on the field vectors by considering the film to be a sheet of surface current. If the refractive index of the substrate is n, and the film thickness d, the coefficients[8] are

$$\mathcal{T}_F = 4n/[(n+1+\Sigma)^2 + \Xi^2], \tag{1a}$$

$$\mathcal{R}_F = \frac{(n-1+\Sigma)^2 + \Xi^2}{(n+1+\Sigma)^2 + \Xi^2} \quad \text{(front)}, \tag{1b}$$

$$\mathcal{R}_F' = \frac{(1-n+\Sigma)^2 + \Xi^2}{(n+1+\Sigma)^2 + \Xi^2} \quad \text{(rear)}, \tag{1c}$$

where $\Sigma = (4\pi/c)\sigma_1 d$ and $\Xi = (\omega/c)(\epsilon_1 - 1)d$. $\mathcal{R}_F$ ($\mathcal{R}_F'$) is used if the radiation is incident on the film from the vacuum (substrate) side.

When the interior wavelength becomes comparable to crystallite size, the film will not be specular and scattering becomes important. The scattering was observed directly by tipping the film in steps away from the specular reflection position; at 4000 cm^{-1}, about 60% of the reflected radiation is scattered out of the 12° acceptance angle of the spectrometer. Thus the measured transmission and reflection ($\mathcal{T}_{FM}$, $\mathcal{R}_{FM}$, and $\mathcal{R}_{FM}'$) are reduced from the ideal values of Eq. (1).

Three independent measurements (transmission, and reflection with radiation incident from front and rear) systematically account for the scattering. We detect only that fraction of transmitted or reflected intensity which is not scattered out of the acceptance angle. By conservation of energy, $1 = \mathcal{A} + \mathcal{R}_{FM} + \mathcal{T}_{FM} + \mathcal{S}$, where $\mathcal{A}$ is the absorption and $\mathcal{S}$ the scattering in the film. Since the scattering depends only on the intensity in the film and the wavelength, a good approximation is $\mathcal{S} = \kappa(\omega)(\mathcal{R}_{FM} + \mathcal{T}_{FM})$, where $\kappa(\omega)$ is the frequency-dependent scattering factor. Thus, the ideal coefficients entering Eq. (1) are

$$\mathcal{T}_F \simeq [1+\kappa(\omega)]\mathcal{T}_{FM}, \quad \mathcal{R}_F \simeq [1+\kappa(\omega)]\mathcal{R}_{FM}, \quad \mathcal{R}_F' \simeq [1+\kappa(\omega)]\mathcal{R}_{FM}'. \tag{2}$$

Equations (1) and (2) form three independent expressions which may be solved for $\sigma_1(\omega)$, $\epsilon_1(\omega)$, and $\kappa(\omega)$, after accounting for multiple reflections in the substrate.

Figure 1 shows the frequency dependence of $\sigma_1(\omega)$ from 0 to 4000 cm^{-1}. Since we are treating the films as an effective medium, the experiment measures the average value of the anisotropic conductivity, $\langle\sigma_1\rangle = \frac{1}{3}(\sigma_1{}^b + \sigma_1{}^a + \sigma_1{}^{c*})$. At all frequencies below the plasma frequency where measurements have been made, the conductivity along the b axis is more than 2 orders of magnitude larger than in the transverse directions.[2-4] Thus, we have plotted $3\langle\sigma_1\rangle$ to make comparison with values obtained from single-crystal measurements. The solid bars indicate the conductivity obtained from dc[1,2] and microwave[3] measurements.[9]

The general form of the conductivity is that of an electronic system with an energy gap $\omega_g \simeq 10^3$ cm^{-1} (0.14 eV). However, both dc and 10-GHz experiments show that the low-frequency intrinsic conductivity $\sigma_1{}^b$ is at 300 K approximately 10^3 $(\Omega\,\text{cm})^{-1}$ and by 65 K exceeds 10^4 $(\Omega\,\text{cm})^{-1}$. Thus, the frequency-dependent conductivity, Fig. 1, indicates the existence of quasiparticle excitations above an energy gap with a collective mode at zero frequency. $\sigma_1(\omega)$ is thus qualitatively

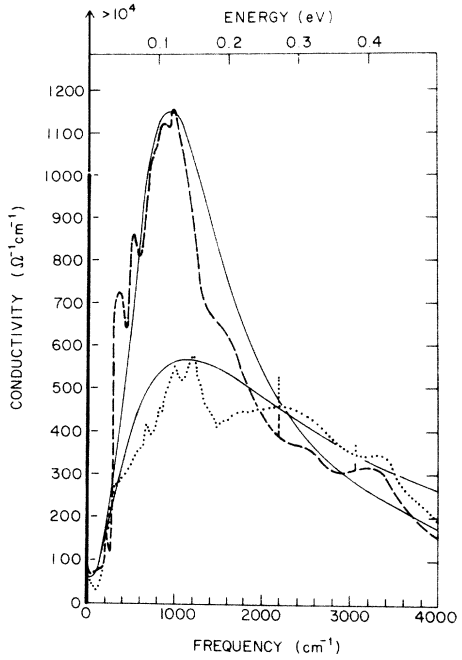

FIG. 1. Conductivity $[3\langle\sigma_1(\omega)\rangle]$ versus frequency in TTF-TCNQ at 65 K (dashed line) and 320 K (dotted line). The solid lines are from Eq. (3). The heavy bars at zero frequency indicate the dc and microwave values, $\sim 10^3$ at 320 K and $> 10^4$ at 65 K.

similar to that obtained from IR studies of superconductors.

As a check we have performed a Kramers-Kronig (K-K) analysis of $\sigma_1(\omega)$ to obtain $\epsilon_1(\omega)$. The results are compared in Fig. 2(a) with values of $\epsilon_1(\omega)$ obtained directly from the point-by-point determination assuming that ϵ_a and ϵ_c are approximately ϵ_{core}. The identical shape of the K-K transform provides evidence that the data analysis is valid. Confirmation that the scattering is properly described by Eq. (2) comes from the scattering factor $\kappa(\omega)$ [Fig. 2(b)], which increases with frequency reaching 54% at 4000 cm^{-1} in quantitative agreement with the tipping experiment. Moreover, polarized reflectivity data (320 K) of single crystals in the region 200–3500 cm^{-1} are in agreement with the reflectivity as calculated from $\sigma_1(\omega)$ and the K-K $\epsilon_1(\omega)$.

Figure 3 gives the far-IR results at 65 and 4.2 K. At 4.2K, the overall magnitude of $\sigma_1(\omega)$ is reduced in the spectral range below 200 cm^{-1}, but the principal feature is the broad maximum centered at 80 cm^{-1}. In addition, several sharp temperature-independent molecular lines are clearly seen as peaks in $\sigma_1(\omega)$.

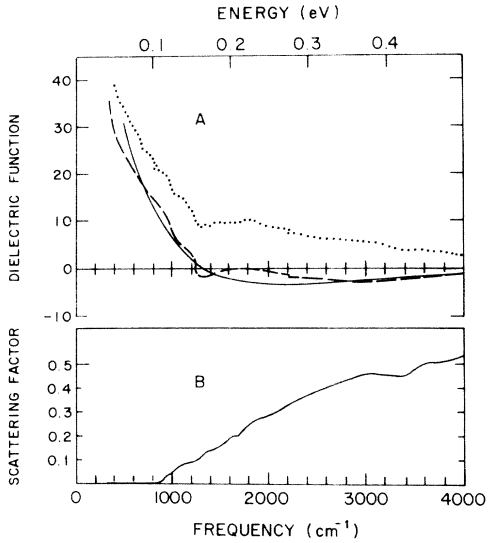

FIG. 2. (a) Dielectric function $[3\langle\epsilon_1(\omega)\rangle - 2\epsilon_{core}]$ versus frequency in TTF-TCNQ at 320 K. Dashed curve, K-K transform of $\sigma_1(\omega)$ from Fig. 1; dotted curve, from Eqs. (1) and (2); solid curve, from Eq. (3). (b) The scattering factor $[\kappa(\omega)]$ versus frequency.

The composite-medium problem was first discussed by Maxwell-Garnett.[10] For a conducting single crystal in a uniform electric field, E_0, the internal field is given by $E_i = E_0[1 + g(\epsilon - 1)]^{-1}$,

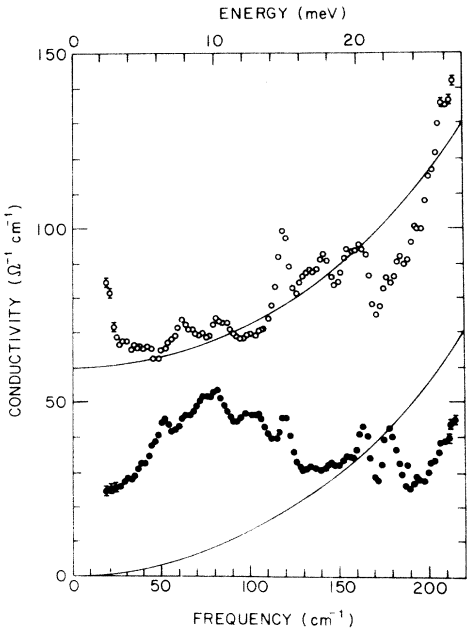

FIG. 3. Conductivity $[3\langle\sigma_1(\omega)\rangle]$ versus frequency: Open circles at 65 K and closed circles at 4.2 K; solid lines from Eq. (3) with $\sigma_M = 0$ at 4.2 K, with $\tau = 7 \times 10^{-15}$ sec.

where g is the depolarization factor. If $g|\epsilon|<1$, then $E_i \approx E_0$, and the loss (σE_i^2) is proportional to σ. In the opposite limit, $E_i \propto E_0 \epsilon_2^{-1}$ and the loss varies as σ^{-1}. For the general case of a medium containing randomly oriented ellipsoids with an anisotropic dielectric function, these limits correspond to the conditions (when the filling factor is of order unity, as for a film) $\frac{8}{3}\pi g \sigma_1^b / \omega\epsilon_\perp \ll 1$ or $\gg 1$, where σ_1^b is the conductivity along the principal conducting axis, and $\epsilon_\perp$ is the transverse dielectric constant. In the first case ($\ll 1$), depolarization effects are unimportant and $\sigma_1^{\text{medium}}(\omega) \simeq \frac{1}{3}\sigma_1^b(\omega)$. In the opposite limit ($\gg 1$), depolarization effects dominate and $\sigma_1^{\text{medium}}(\omega) \simeq 3(\omega\epsilon_\perp/8\pi g)^2/\sigma_1^b(\omega)$. Taking $\epsilon_\perp > 10$, $g \simeq 10^{-2}$, and $\sigma_1^b \simeq 60$ $(\Omega\ \text{cm})^{-1}$ (see Fig. 3), one estimates the crossover frequency, $\omega_c < 0.2\ \text{cm}^{-1}$, well below the frequency range covered. Interparticle capacitive shorting inhibits charge buildup and lowers ω_c even more. We note that if σ_1 increases, as is the case near a molecular resonance, σ_1^{medium} also increases only if $\omega > \omega_c$. Since in Fig. 3 the molecular modes are resonances and not antiresonances (note particularly the sharp line at 120 cm^{-1} known to be polarized within 30° of the conducting axis), the limit $\sigma_1^{\text{medium}} \simeq \frac{1}{3}\sigma_1^b$ applies throughout the experimental frequency range.

Above 58 K, $\sigma_1(\omega)$ in the far IR is approximately 60 $(\Omega\ \text{cm})^{-1}$. We understand this in terms of the two-chain model in which one set of chains is metallic (σ_M) while the other is in the dynamically distorted Peierls-Fröhlich state.[5-7] The data of Fig. 1 suggest that the low-frequency conductivity is associated with the metallic chain, $\sigma_M \sim 60$ $(\Omega\ \text{cm})^{-1}$. However, the dc conductivity is dominated by the collective mode.

Because of the large energy gap, a description of $\sigma_1(\omega)$ must include direct transitions across the gap and indirect transitions involving multiple phonon processes which give rise to the Drude absorption in metals. We approximate the frequency-dependent conductivity with a Drude-Lorentz model appropriate to a 1D system with a large density-of-states peak at the band edge (plus σ_M):

$$\sigma(\omega) = \frac{\omega}{4\pi}\left[\frac{\omega_p^2 \tau}{\omega - i(\omega_g^2 - \omega^2)\tau}\right] - \frac{i\omega}{4\pi}(\epsilon_{\text{core}} - 1) + \sigma_M. \quad (3)$$

The solid lines in Figs. 1, 2, and 3 represent fits of Eq. (3) to the data with $\omega_p = 9560\ \text{cm}^{-1}$ and $\epsilon_{\text{core}} = 2.4$.[4] On cooling, ω_g decreases from 1150 cm^{-1} (320 K) to 950 cm^{-1} (65 K), and the single-particle scattering time τ at high frequencies increases from 1.8×10^{-15} sec (320 K) to 3.8×10^{-15} sec (65 K).[11] The temperature dependence of τ and the Drude form above 2000 cm^{-1} are consistent with the single-crystal reflectivity measurements.[4]

According to Lee, Rice, and Anderson,[8] the giant density-wave collective mode will be pinned below the 3D ordering temperature, leading to a metal-insulator transition, and the collective-mode contribution to σ_1 will shift away from zero frequency to a characteristic pinning frequency ω_T. Earlier studies[1-3,12,13] do show a transition near 58 K below which the conductivity falls dramatically. We identify the broad maximum centered at 80 cm^{-1} in the low-temperature data (Fig. 3) as the pinned collective mode. The total oscillator strength in this maximum corresponds to an effective mass[5-7] of about 300 times the band mass, and agrees in order of magnitude with our estimate of the collective-mode contribution at 65 K based on the magnitudes of $\sigma_1(0)$ and σ_1(10 GHz) and the far-IR data. The low-temperature microwave results,[3] showing the conductivity exceeding dc values by 3 orders of magnitude, are understood as resulting from the tail of the 80-cm^{-1} broad maximum. Thus, the experiments yield direct evidence for the pinning of the collective mode at low temperatures.

Our present understanding of the data[14] is based on 1D fluctuations of a Peierls-Fröhlich dynamically distorted state at temperatures well below the Peierls temperature. Using the conventional mean-field result, $\hbar\omega_g = 3.5 k_B T_P$, with $\omega_g = 1050 \pm 100\ \text{cm}^{-1}$, we obtain $T_P = 430$ K, in reasonable agreement with estimates of T_P from other measurements.[2,4,7] In conclusion, the results of this study suggest that TTF-TCNQ is a 1D Fröhlich superconductor with a mean-field transition temperature of 400–500 K.

We thank Professor E. Nixon and Professor E. Burstein for use of their facilities.

*Supported by the National Science Foundation and the Advanced Research Projects Agency.

†Predoctoral fellow, Technical University of Denmark; work supported in part by a grant from the Danish Research Council.

[1]L. B. Coleman, M. J. Cohen, D. J. Sandman, F. G. Yamagishi, A. F. Garito, and A. J. Heeger, Solid

State Commun. 12, 1125 (1973).
[2]M. J. Cohen, L. B. Coleman, A. F. Garito, and A. J. Heeger, Phys. Rev. B (to be published).
[3]S. K. Khanna, E. Ehrenfreund, A. F. Garito, and A. J. Heeger, to be published.
[4]A. A. Bright, A. F. Garito, and A. J. Heeger, Phys. Rev. B (to be published).
[5]H. Fröhlich, Proc. Roy. Soc., Ser. A. 223, 296 (1954).
[6]J. Bardeen, Solid State Commun. 13, 357 (1973); D. Allender, J. W. Bray, and J. Bardeen, Phys. Rev. B 9, 119 (1974).
[7]P. A. Lee, T. M. Rice, and P. W. Anderson, Phys. Rev. Lett. 31, 462 (1973), and to be published.
[8]L. N. Hadley and D. M. Dennison, J. Opt. Soc. Amer. 37, 451 (1947); L. H. Palmer and M. Tinkham, Phys. Rev. 165, 1588 (1968).
[9]The fine structure arises from molecular vibrational modes (e.g., C-N stretch at 2200 cm^{-1}, C-H stretch at 3070 cm^{-1}, and C=C stretch at 1500 cm^{-1}).
[10]J. Maxwell-Garnett, Phil. Trans. Roy. Soc. (London) 203, 385 (1904), and 205, 237 (1906).
[11]Below 200 cm^{-1}, $\tau \simeq 7\times 10^{-15}$ sec at 65 and 4.2 K. The longer time is expected at low frequencies where phonon emission is not allowed.
[12]J. Ferraris, D. O. Cowan, V. Walatka, and J. H. Perlstein, J. Amer. Chem. Soc. 95, 948 (1973).
[13]R. A. Craven, M. B. Salomon, G. DePasquali, R. M. Herman, G. Stucky, and A. Schultz, Phys. Rev. Lett. 32, 769 (1974).
[14]J. B. Torrance and D. F. Nicoli [Bull. Amer. Phys. Soc. 19, 336 (1974)] have presented data on $\sigma_1(\omega)$ for small TTF-TCNQ crystals compacted into KBr which are in qualitative agreement with those presented here.

Multiphonon Optical Spectrum of NaF

Thomas F. McNelly* and Dieter W. Pohl
IBM Zurich Research Laboratory, 8803 Rüschlikon, Switzerland
(Received 25 March 1974)

The high-frequency exponential wing of the reststrahlen band of NaF is decomposed into a number of N-phonon absorption spectra ($N=2,3,4,5$) by means of a temperature analysis. Overall agreement of the individual spectra with recent theoretical predictions is good, except for a fairly pronounced structure which indicates particularly strong contributions from certain frequencies of the TO and LO phonon branches.

The infrared (i.r.) multiphonon spectrum of many ionic crystals is characterized by a uniform, almost exponential, decay of absorption with frequency.[1] The lack of distinct peaks at the main combination frequencies (like in homopolar crystals) prevents conclusions on the number of participating phonons from the shape of the spectrum alone. The mechanisms responsible for the unstructured wing absorption have recently attracted considerable theoretical attention.[2,3] Various classical and quantum-mechanical approaches with different assumptions for the interionic potential and the phonon dispersion were used to explain this phenomenon.

A key to the experimental identification of the various multiphonon processes is the temperature dependence of the absorption.[4-6] The larger the number N of phonons participating, the steeper the increase of absorption α_N with temperature. For this reason we made a systematic analysis of the i.r. properties of NaF between 600 and 1500 cm^{-1} and from 100 to 850°K. The obtained data yield empirical probabilities for N-phonon processes, $N=2$, 3, 4, 5, and 6, which, for the first time, allow an experimental decomposition of the multiphonon wing into a series of N-phonon spectra. In this way a much more direct control of theoretical predictions becomes possible.

Two NaF samples [(A) 54.98 mm,[7] and (B) 3.82 mm,[8] thickness] of extreme purity were employed. There were no indications of any extrinsic absorption which is important in view of the very small absorption at large frequencies. The crystals were mounted either in a cryostat (90 to 400 400°K) or in a small oven (300 to 850°K). The absorption was measured by means of a Beckman Acculab-6 i.r. spectrophotometer. Values of the transmission between 1 and 98–99% could be well detected. The corresponding absorption ranges from about 10 cm^{-1} down to less than 0.002 cm^{-1}. At temperatures different from ambient, corrections to the measured nominal transmission were required. The instrument was not compensated for the thermal radiation from the sample with respect to the variable attenuator in the reference beam. Knowledge of the source characteristic,[9] i.e., its temperature (1240°K)